AIP | Journal of Applied Physics

Interaction of shear-coupled grain boundary motion with crack: Crack healing, grain boundary decohesion, and sub-grain formation

Mohammad Aramfard and Chuang Deng

Citation: Journal of Applied Physics **119**, 085308 (2016); doi: 10.1063/1.4942842
View online: http://dx.doi.org/10.1063/1.4942842
View Table of Contents: http://scitation.aip.org/content/aip/journal/jap/119/8?ver=pdfcov
Published by the AIP Publishing

JOURNAL OF APPLIED PHYSICS **119**, 085308 (2016)

Interaction of shear-coupled grain boundary motion with crack: Crack healing, grain boundary decohesion, and sub-grain formation

Mohammad Aramfard and Chuang Deng[a)]
Department of Mechanical Engineering, University of Manitoba, 15 Gillson Street, Winnipeg, MB R3T 5V6, Canada

(Received 2 November 2015; accepted 13 February 2016; published online 29 February 2016)

Stress-driven grain boundary motion is one of the main mechanisms responsible for microstructural evolution in polycrystalline metals during deformation. In this research, the interaction of shear-coupled grain boundary motion (SCGBM) in face-centered cubic metals with crack, which is a common type of structural defects in engineering materials, has been studied by using molecular dynamics simulations in simple bicrystal models. The influences of different parameters such as metal type, temperature, grain boundary structure, and crack geometry have been examined systematically. Three types of microstructural evolution have been identified under different circumstances, namely, crack healing, grain boundary decohesion, and sub-grain formation. The underlying atomistic mechanisms for each type of SCGBM-crack interaction, particularly grain boundary decohesion and crack healing, have also been examined. It is found that crack healing is generally favoured during the SCGBM-crack interaction at relatively high temperature in metals with relatively low stacking fault energy and grain boundary structure with relatively low misorientation angles. The results of this work may open up new opportunities for healing severely damaged materials. © *2016 AIP Publishing LLC*.
[http://dx.doi.org/10.1063/1.4942842]

I. INTRODUCTION

Grain boundary (GB) motion plays important roles in the microstructural evolution in almost every class of polycrystalline materials. In particular, stress-driven grain boundary motion (SDGBM)[1–7] may outweigh dislocation activities in dominating the plasticity and microstructural evolution in nanocrystalline materials during mechanical deformation due to their high volume fraction of GBs. For example, Legros *et al.*[6] have reported based on *in-situ* TEM that extensive GB migration occurs during the *in situ* loading of free standing nanocrystalline Al thin film, which precedes dislocation activity. The *in situ* TEM study on ultrafine-grained Al thin films by Mompiou *et al.*[7] also revealed stress-assisted GB migration along with dislocation emission inside the grain. However, the past studies on SDGBM from either simulations or experiments mainly focused on samples containing no or few structural defects, which are necessary in order to explore some of the most fundamental mechanisms of SDGBM, for example, shear-coupled GB motion (SCGBM).[8,9] Nevertheless, engineering materials in service are rarely defect-free. Among all possible structural defects in engineering materials, cracks are of particular interests since cracks are most common and can dramatically shorten the service life of materials.[8–10] For example, the stress intensity factor can easily increase and reach the critical stress intensity factor for the onset of rapid failure in a material by increasing the crack length.[11] Therefore, it is of dramatic interests for both fundamental research and practical applications to investigate how SDGBM interacts with cracks.

It has been recently reported based on molecular dynamics (MD) simulations that cracks can serve as pinning obstacles to SCGBM, which can cause the bulge of the moving GB and even the formation of sub-grains.[12] On the other hand, crack healing has also been reported during the SCGBM-crack interaction. Crack healing and strength recovery is an interesting phenomenon that has been initially reported in polycrystalline ceramics.[13–15] For example, Gupta showed experimentally that pores and cracks developed by thermal shock in alumina were healed by heat treatment, which was believed to be mediated by GB diffusion.[13] Crack healing by SCGBM-crack interaction, in contrast, requires no heat treatment. Xu and Demkowicz showed from MD simulations that confined SCGBM in Ni can remotely influence a crack and heal it by disclination mediation.[16] Furthermore, SCGBM may also cause intergranular crack propagation or GB decohesion.[17–23] For instance, Adlakha *et al.* investigated the behaviour of a crack in the middle of ⟨1 0 0⟩ and ⟨1 1 0⟩ GBs in a bicrystal model under tension[17,24] and found a correlation between GB structure and the crack growth rate, the maximum stress and other phenomena such as twinning and dislocation nucleation. They suggested that GBs with more free volume have higher crack growth rate during cleavage.

The aim of this work is to systematically investigate the interaction of SCGBM with cracks by using MD simulations. The competition between three observed mechanisms, namely, crack healing, GB decohesion, and new sub-grain formation, in model systems of various face-centered cubic (FCC) bicrystal metals is studied by varying the metal type, GB structure, and temperature. The underlying atomistic mechanisms for each type of SCGBM-crack interaction, particularly grain boundary decohesion and crack healing, are

[a)]Author to whom correspondence should be addressed. Electronic mail: dengc@ad.umanitoba.ca. Tel.: +1 (204) 272-1662.

also examined, which are expected to shed some light on new methods of healing severely damaged materials.

II. METHODOLOGY

All simulations were performed by using open-source software LAMMPS[25] with embedded-atom method potentials for Ag,[26] Al,[27] Au,[28] Cu,[29] and Ni,[30] respectively. Bicrystal models were built with dimensions of $80a \times 7a \times 100a$ (a: lattice constant) along x-, y-, and z-directions, as shown in Figure 1(a). The time step was 5 fs. All models were relaxed at the desired temperature using Nose-Hoover isobaric thermostat (NPT) for 100 ps (Refs. 31 and 32) prior to any deformation. To apply shear deformation, a thin slab of atoms at the top of each model was moved to the right at a constant velocity of $1\,ms^{-1}$ while the lower slab was held fixed. The atomistic configurations were visualized using AtomEye.[33] As a representative, Figure 1(a) shows the Cu Σ29 (3 7 0) bicrystal model with a $10a \times 5a$ elliptical crack at a distance about $\sim 4a$ above the GB. Periodic boundary conditions were applied in the directions parallel to the GB plane while the direction perpendicular to GB plane was set free in the simulation cell. In this work, four types of ⟨1 0 0⟩ symmetric tilt GBs, namely, Σ29 (3 7 0), Σ57 (2 7 0), Σ5 (1 3 0), and Σ5 (1 2 0), were studied. Crystal defects were visualized using Common Neighbor Analysis (CNA)[34] with dark blue atoms corresponding to perfect FCC stacking, red atoms corresponding to GB and point defects, and light blue ones corresponding to stacking faults and dislocations. The six components of stress in every model was calculated by Virial method and averaged over the whole model.[35]

III. RESULTS

A. Influence of temperature on SCGBM-crack interaction

Shear deformation in all bicrystal models has been simulated at temperatures 10 K, 300 K, and 500 K, respectively. As representatives to demonstrate the effects of temperature, Cu bicrystal models with Σ29 (3 7 0) GB after the SCGBM-crack interaction at 10 K, 300 K, and 500 K are shown in Figures 1(b)–1(d). As shown in Figure 1(b), the GB has moved up due to shear-coupling and become pinned at the crack after 10 ns of shear deformation at 10 K. Partial dislocations and twin boundaries were nucleated, which resulted in the formation of sub-grains. The crack was deformed, but no significant healing (shrinkage) or growth was observed. This process is very similar to that has been proposed in the past to describe grain refinement in materials during severe plastic deformation based on dislocation activities,[36–39] i.e., dislocation walls appear during the early stage of plastic deformation, which become low-angle GBs as the deformation continues. Upon further deformation, the newly formed grains rotate and the misorientation angles of low-angle GBs increase, which eventually results in the formation of high-angle GBs.[36–39] In contrast, no dislocations appeared after 10 ns of shear deformation in this model at 300 K. As shown in Figure 1(c), the crack has propagated along the GB from left which enlarged the crack. On the other hand, after 6.7 ns of shear deformation at 500 K, the crack was completely healed and absorbed by the GB, leaving a wavy GB in the model (Figure 1(d)). Figure 1 thus clearly shows three dramatically different mechanisms from low to high temperature, i.e., sub-grain formation (10 K), crack growth (300 K), and crack healing (500 K), caused by the interaction of SCGBM and crack in the same structure. However, it is important to mention that although temperature has a huge influence on the SCGBM-crack interaction, the dominating mechanism during the SCGBM-crack interaction also strongly depends on the GB structure and metal types, as shown below.

B. Influence of GB structure on SCGBM-crack interaction

Four bicrystal models containing a high-angle symmetric tilt GB with misorientation angle ranging from 31.9° (Σ53 (2 7 0)) to 53.1° (Σ5 (1 2 0)) in Cu at 500 K were presented in Figure 2 to show the influence of GB structure on the interaction of SCGBM with crack. Here, the four special GBs were chosen for showing relatively strong shear coupling effects.[40] As having been presented in Figure 1(d), the bicrystal model containing Σ29 (3 7 0) GB (misorientation angle = 46.4°) showed complete crack healing at 500 K after 6.7 ns of shear deformation (Figure 2(a)). Similarly, the model with Σ53 (2 7 0) GB also showed complete crack healing but with some residual dislocations after 9.15 ns of shear deformation (Figure 2(b)). In contrast, the models with Σ5 (1 2 0) and Σ5 (1 3 0) GBs showed different behaviors. Specifically, a new sub-grain was formed in the region surrounded by the bent GB and crack after the GB was bulged over the crack in the model containing Σ5 (1 2 0) GB (Figure 2(c)). The crack was deformed but with no significant healing or growth. This phenomenon was due to the

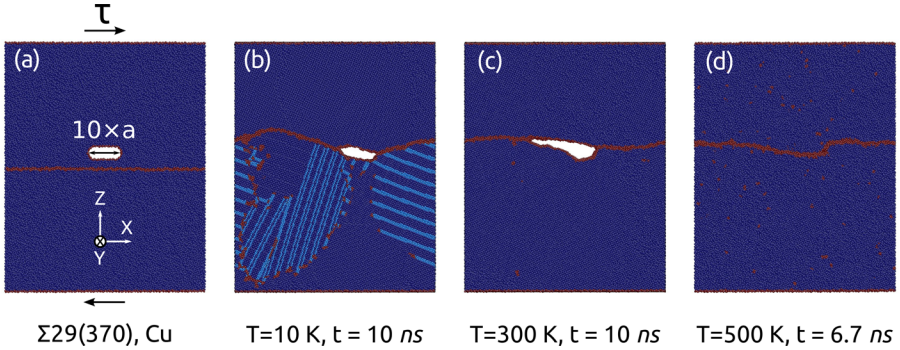

FIG. 1. Cu Σ29 (3 7 0) bicrystal model containing elliptic crack deformed by shear. (a) Undeformed model, deformed model at (b)10 K after 10 ns, (c) 300 K after 10 ns, and (d) 500 K after 6.7 ns of shear deformation.

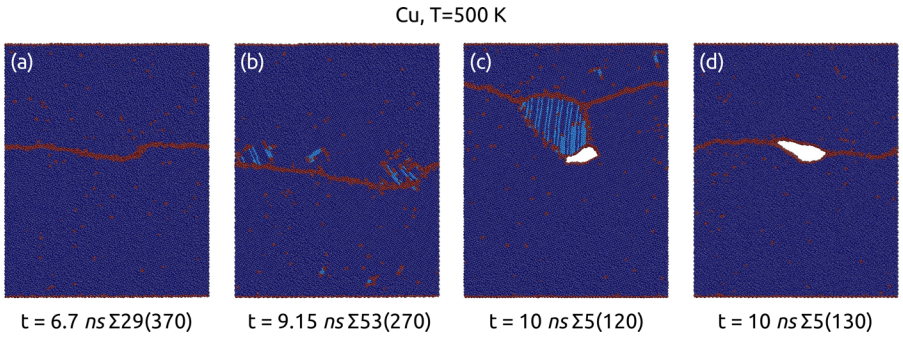

FIG. 2. Influence of GB type on the SCGBM-crack interaction. Cu bicrystal model at 500 K with (a) Σ29 (3 7 0) GB after 6.7 ns, (b) with Σ53 (2 7 0) GB after 9.15 ns, (c) with Σ5 (1 2 0) GB after 10 ns, and (d) with Σ5 (1 3 0) GB after 10 ns of shear deformation.

formation of disclination quadrupoles, which has been explained in details elsewhere.[12] The model with Σ5 (1 3 0) GB, however, showed severe GB decohesion, which enlarged the crack during the SCGBM-crack interaction (Figure 2(d)). Although only four types of special GBs were investigated, the results in Figure 2 suggest that the GB structure has a strong influence on the SCGBM-crack interaction. This finding is in agreement with previous work on the dependence of crack initiation and propagation on GB type.[24] For example, Adlakha *et al.* have reported for selected ⟨1 0 0⟩ GBs that the initial free volume and structural units of GB influences the normal strength and crack propagation rate of the crack embedded in the GB under tensile deformation. They found that Σ13 (5 1 0) GB, which has "D" structural unit, and Σ97 (9 4 0) GB, which has the highest free volume, showed more crack propagation and lower normal stress than other GBs.[24]

C. Influence of metal type on SCGBM-crack interaction

To examine the influence of metal type on SCGBM-crack interactions, five types of FCC metals, i.e., Ag, Al, Au, Cu, and Ni, were examined. The representative results from models containing a Σ29 (3 7 0) GB deformed at 500 K in each metal are shown in Figure 3. It can be clearly seen that depending on the metal type, the crack could heal, grow, or show a combination of both. Specifically, Al and Ni showed significant crack growth and propagation along the GB (Figures 3(b) and 3(e)) which suggests that metals with relatively high stacking fault energy (SFE) tend to deform by cleavage during SCGBM-crack interaction. On the other hand, Cu and Au showed complete crack healing, after which a wavy GB was left (Figures 3(c) and 3(d)). In contrast, Ag which has the lowest stacking fault energy[26] modeled in this study showed partial crack healing at the beginning, which was followed by crack growth later on due to GB decohesion (Figure 3(a)); the whole process is shown in supplementary movie S1[41] by using Ovito.[42] Crack healing followed by crack growth was also observed in Ag with Σ53 (2 7 0) GB deformed at 300 K. As shown in supplementary movie S2,[41] the crack first completely healed, but GB decohesion occurred afterwards in a highly wavy region of the GB. By varying the temperature and GB structure, sub-grain formation was also observed in Ag Σ5 (1 2 0) at all temperatures and Au Σ5 (1 3 0) and Σ5 (1 2 0) at 10 K. All the observed mechanisms during SCGBM-crack interaction simulated in this research are summarized in Table I.

Overall, SFE was found to play a key role in activating different mechanisms that can occur during the SCGBM-crack interaction. Specifically, metals with relatively high SFE tend to show decohesion while metals with relatively low SFE tend to hinder crack propagation and show crack healing or sub-grain formation. For example, in all the Cu bicrystal models, no significant crack growth (or GB decohesion) was observed regardless the temperature and GB type. On the contrary, Table I shows that Al and Ni models showed GB decohesion in all cases. However, it is important to mention that since each EAM potential may be developed and fitted for different purposes, SFE energy may not be the only parameter that may influence the SCGBM-crack interaction observed in our simulations for different metals.

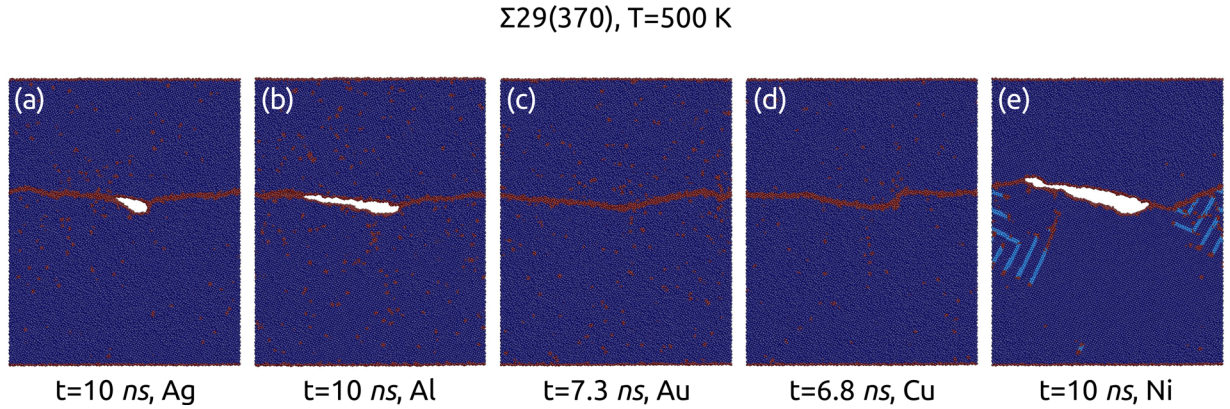

FIG. 3. Influence of material type on SCGBM-crack interaction. Bicrystal models containing Σ29 (3 7 0) GB deformed at 500 K in (a) Ag, (b) Al, (c) Au, (d) Cu, and (e) Ni.

TABLE I. Summary of SCGBM-crack interaction mechanisms: decoh = GB decohesion; sub-grain = sub-grain formation; heal = crack healing; and shrn = crack shrinkage (partial healing). Mechanism a/mechanism b: mechanism *a* followed by mechanism *b*. *Crack did not shrink or propagate, **crack healed but GB became decoherent at other location; #GB traveled in other direction and did not reach crack. Dual behaviour of Σ53 (2 7 0) has been reported in Ref. 40.

GB type	Σ5 (1 2 0)			Σ5 (1 3 0)			Σ29 (3 7 0)			Σ53 (2 7 0)		
T (K)	10 K	300 K	500 K	10 K	300 K	500 K	10 K	300 K	500 K	10 K	300 K	500 K
Metal (SFE mJ m^{-2})												
Ag (1.5)[a]	Decoh/ sub-grain	Shrn/ sub-grain	Shrn/ sub-grain	Decoh/ sub-grain	Decoh	Decoh	Heal	Decoh	Decoh	Decoh	Heal/decoh**	Heal
Al (127)[b]	Decoh	Decoh	Decoh	Decoh	Decoh	Decoh	Decoh	Decoh	Decoh	Decoh	Decoh	Decoh
Au (41)[c]	Heal/ sub-grain	Shrn	Decoh	Decoh/ sub-grain	Decoh	Shrn	None*	Heal	Heal	Heal	Heal	None#
Cu (40)[d]	Sub-grain	Sub-grain	Decoh/ sub-grain	Decoh/ sub-grain	Decoh	Decoh	Decoh/ sub-grain	Decoh	Heal	Decoh	Decoh	Heal
Ni (193)[e]	Decoh/ sub-grain	Decoh/ sub-grain	Decoh/ sub-grain	Decoh	Decoh	Decoh	Decoh/ sub-grain	Decoh/ sub-grain	Decoh/ sub-grain	Decoh/ sub-grain	Decoh/ sub-grain	Decoh

[a]Reference 26.
[b]Reference 27.
[c]Reference 28.
[d]Reference 29.
[e]Reference 30.

D. Stress-strain analysis during SCGBM-crack interaction

Representative shear stress vs. shear strain curves of the Cu models containing Σ5 (1 2 0), Σ5 (1 3 0), and Σ29 (3 7 0) GBs at 500 K are shown in Figure 4, which correspond to sub-grain formation, crack growth, and crack healing, respectively. All the three GBs showed stick-slip behavior before the GB reached the crack. However, the two Σ5 GBs showed higher threshold to initiate the shear-coupled GB motion than the Σ29 GB. Upon reaching the crack, the stress required to activate the three different mechanisms, from low to high, was for crack healing (~500 MPa, Σ29 (3 7 0) GB), crack growth (~700 MPa, Σ5 (1 3 0) GB), and sub-grain formation (~1400 MPa, Σ5 (1 2 0). It is worth mentioning that in the model with Σ5 (1 3 0) GB, the crack growth temporarily paused at ~0.17 strain and restarted when the stress reached ~900 MPa at ~0.23 strain. It is suggested by comparing these curves that there is a competition between the three mechanisms and all of them will relieve the stress in the model once activated. However, which mechanism will eventually dominate depends on multiple parameters including temperature, GB structure, metal type, and even the geometry of the crack. It is suggested based on the previous results that cracks tend to be healed at relatively high temperature in metals with low to moderate stacking fault energy and GBs of relatively small misorientation. A more accurate model to predict the prevailing mechanisms during the SCGBM-crack interaction, however, is currently not available mainly due to the large parameter space of GBs; future study is needed to exhaust as many GB types as possible.

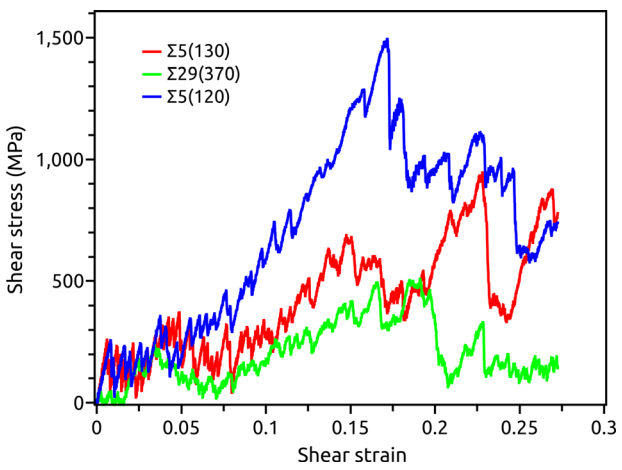

FIG. 4. Shear stress vs. shear strain curves of Cu showing crack healing, sub-grain formation, and GB decohesion at 500 K.

IV. DISCUSSION

A. Atomistic mechanism of crack healing

So far, we have shown that the interaction of SCGBM with crack can result in three different mechanisms and there is a close competition between them. Since crack healing is of practical importance for engineering materials, it is necessary to explore the underlying mechanism of crack healing from the microstructural point of view. As a representative, Figure 5 shows two snapshots of the atomic configuration of Ag Σ29 (3 7 0) model prior to and during the crack healing at 10 K. Specifically, Figure 5(a) shows the snapshot when the GB reached the crack. It is noticed that although the GB became pinned at both ends of the crack, the pinning point on the right side moved up along with the GB while the pinning point on the left side was almost immobile. This asymmetric pinning effect of crack to a moving GB is consistent with previous findings,[43] which played an important role during the healing of the crack. Due to the asymmetric pinning effect, the crack was divided into upper and lower parts. The lower part moved to left while the upper part moved to right during the shear deformation, which makes the two parts of

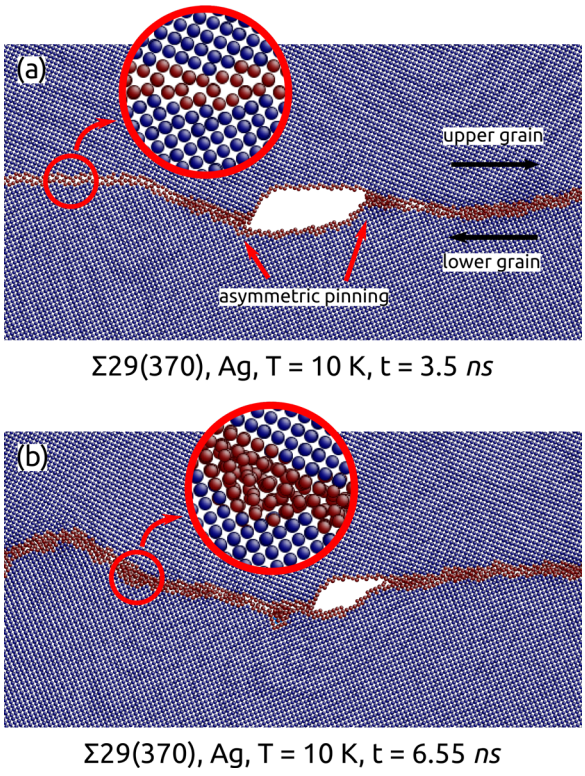

FIG. 5. Atomistic mechanism of crack healing in Ag Σ29 (3 7 0) deformed at 10 K. (a) Asymmetric pinning effect of GB upon reaching crack. (b) Transformation of GB structure during SCGBM-crack interaction. The inset in (a) shows initial structure of GB, and the inset in (b) shows structure of the GB after transformation.

the crack to be pushed together and hence to be closed. However, in order to completely heal a crack, the free volume of the crack has to be absorbed by the GB, which would inevitably transform the GB structure. The original flat symmetric tilt GBs are consisted of structural units as shown in the inset of Figure 5(a). It can be seen clearly from the inset of Figure 5(b) that the transformed GB has a more disordered structure with significant atom shuffling and larger thickness than the original flat Σ29 (3 7 0) GB, which could accommodate more free volume. In addition, the transformed GB became wavy, which dramatically increased the total GB area and the ability to host free volumes.

It is also important to mention that partial healing occurred in the right part of the crack during the early stage of the SCGBM-crack interactions in all simulations regardless of the temperature, GB structure, or metal types. Figure 6 shows the normal stress (σ_{zz}) distribution of three representative

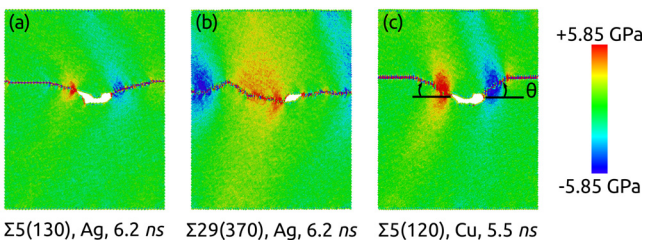

FIG. 6. σ_{zz} distribution in the models of (a) Ag Σ5 (1 3 0) showing GB decohesion, (b) Ag Σ29 (3 7 0) showing crack healing, and (c) Cu Σ5 (1 2 0) showing sub-grain formation.

models, which showed crack growth (GB decohesion), crack healing, and sub-grain formation, respectively. If we define the angle between the GB and the horizontal plane (θ), as shown in Figure 6(c), it can be found that when the angle is positive (clock-wise) the stress acting on the region around the crack tip is tensile and vice versa. Due to the pinning effect, the GB became bent during the SCGBM-crack interaction and showed non-uniform stress distribution. Specifically, the GB area around the crack tip is under compression (blue color) on the right side and under tension (red color) on the left side.

The compressive stress around the crack tip is therefore responsible for the partial healing of the crack in all models at the very beginning of the SCGBM-crack interaction. In contrast, tensile stress around the crack tip will potentially contribute to crack growth or GB decohesion. However, since it is expected that a threshold stress needs to be achieved in order to initiate GB decohesion (or to "open up" the crack),[24] which depends on the GB structure, temperature, and metal type, the tensile stress cannot always cause crack growth. The tensile stress around the bent GB may also be relieved by transforming the GB structure and becoming flat by absorbing free volumes (see supplementary Movie S3[41]), which has also been reported before by Frolov *et al.* based on MD simulations.[44,45]

B. Comparison between atomistic mechanisms of crack healing and GB decohesion

The sub-grain formation process, for example, in the Cu model with Σ5 (1 2 0) GB at 10 K (Figure 6(c)), was due to the formation of disclinations during the SCGBM-crack interaction, which has been discussed in detail elsewhere.[12] Therefore, the following discussion will mainly focus on the comparison between GB decohesion and crack healing by using Al model with Σ5 (1 3 0) GB at 10 K (Figures 7(a)–7(c)) and Ag model with Σ29 (3 7 0) GB at 10 K (Figure 7(d)–7(f)) as examples, respectively. The original flat Σ5 (1 3 0) GB is consisted of discontinuous "A" kite-shape structure units as shown by solid lines in Figure 7(a). Due to SCGBM, part of the GB was pinned at crack tips and become inclined. The kite-shape units of the inclined GB have slightly different microstructure than the original flat GB, which are "two-by-two" and "back-to-back." To open up the crack along the GB, two back-to-back units act together, which are indicated as "1" and "2" in Figures 7(a)–7(c) at the crack tip. Based on the stress analysis in Figure 6, the inclined structure has a positive (clockwise) angle, which should experience tensile stress during the shear deformation. The unit "1" and "2" started to "unzip" consecutively when the tensile stress reached a threshold. In contrast, the Σ29 (3 7 0) GB as shown in Figure 7(d) is consisted of mated "A" structural units (flat part of GB in Figure 7(a)) that makes this GB to be harder to unzip than the Σ5 (1 3 0) GB. In addition, Ag has significantly lower SFE than Al. It is therefore expected that Ag atoms at the GB are easier to shuffle than Al, which would hinder the crack from propagation and consume the free volume of the crack (see Figures 7(d)–7(f)).

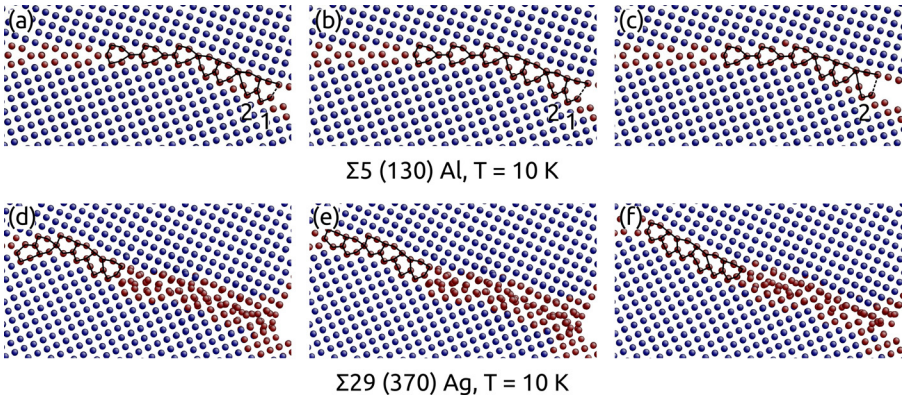

FIG. 7. Atomistic structure of (a)–(c) Al with Σ5 (1 3 0) GB and (d)–(f) Ag with Σ29 (3 7 0) GB deformed at 10 K during SCGBM-crack interactions.

C. Influences of crack geometry during SCGBM-crack interaction

The geometry of the crack has also influences on which mechanism to prevail during SCGBM-crack interaction. Figure 8 shows the circular voids with diameter of 8 *a* embedded in a Cu bicrystal model with Σ5 (1 2 0) GB. Although the volume of these circular voids is larger than the elliptic cracks in previous models, they can be healed more easily than the elliptic ones. For example, the Cu model with Σ5 (1 2 0) GB at 300 K showed sub-grain formation instead of complete crack-healing with elliptic cracks, but the same model with circular cracks can be healed completely also at 300 K during SCGBM-crack interactions, as shown in Figures 8(a)–8(c). A key process of the crack healing shown in Figure 8 is still the asymmetric pinning effects; the left junction of GB and void became significantly lower than the right one due to SCGBM-crack interaction. Considering the size of the cracks relative to the total volume of the model shown in Figure 8, it is expected that SCGBM-crack interactions may be utilized as an effective approach to heal heavily damaged engineering materials.

It is worth mentioning again that the results presented in this work are based on only five different FCC metals and four types of symmetric tilt GBs. Although MD simulations have the advantage of being more economic than experiments to construct and test a specific type of metal and GB, it is not possible to explore all random and general GBs. Furthermore, since MD simulations are limited by the length and time scale and no impurity or vacancies are considered in this research, experimental validation is needed to test if the predicted mechanisms of crack healing, crack growth, or sub-grain formation can be extended to engineering materials in the real world. For example, Miura has recently observed the bulging of GB and nucleation of new sub-grains at bulged GBs and triple junctions in Cu bicrystal, tricrystal, and polycrystal models under stress,[45] which partially supported the findings from our MD simulations. Nevertheless, the results presented here can be regarded as a step forward to find new ways of healing and optimizing structures that are heavily damaged during processing or service.[46,47]

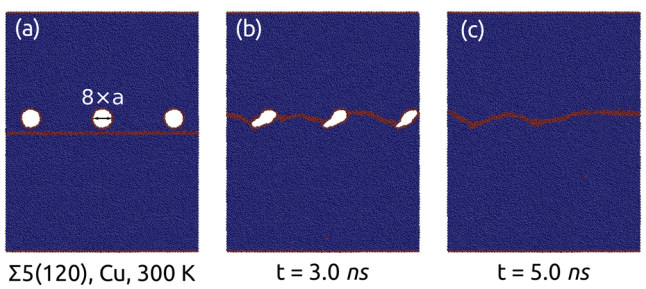

FIG. 8. Interaction of circular voids with Σ5(120) GB in Cu deformed at 300 K. (a) The initial configuration, (b) the configuration after 3.0 ns of deformation, and (c) the configuration showing complete void healing after 5.0 ns of deformation.

V. CONCLUSIONS

A new crack healing mechanism in metals was found by using MD simulations which is facilitated by the interaction of SCGBM and crack. During the SCGBM-crack interaction, the free volumes could be consumed by transforming the GB structure, which facilitates the crack healing process. This mechanism competes with two other mechanisms, i.e., crack propagation along GB and sub-grain formation, and which mechanism will prevail depends on temperature, the GB structure, and the metal type. It is suggested based on the results from this work that crack healing can be activated more easily in metals at high temperature with relatively low stacking fault energy and GB structure with relatively low misorientation angles. The findings from this research may be utilized to design new ways of healing heavily damaged engineering materials.

ACKNOWLEDGMENTS

The authors are sincerely thankful for the support from Professor Christopher Schuh at Massachusetts Institute of Technology, USA, and an NSERC Discovery Grant under RGPIN 430800-2013, Canada. This work was performed by the use of computing resources provided by WestGrid and Compute/Calcul Canada.

[1]T. J. Rupert, D. S. Gianola, Y. Gan, and K. J. Hemker, Science **326**, 1686 (2009).
[2]D. Wolf, V. Yamakov, S. R. Phillpot, A. Mukherjee, and H. Gleiter, Acta Mater. **53**, 1 (2005).
[3]J. Schiøtz and K. W. Jacobsen, Science **301**, 1357 (2003).
[4]J. Schiøtz, F. D. D. Tolla, and K. W. Jacobsen, Nature **391**, 561 (1998).
[5]A. P. Sutton and R. W. Balluffi, *Interfaces in Crystalline Materials* (Clarendon Press, 1995).

[6]M. Legros, D. S. Gianola, and K. J. Hemker, Acta Mater. **56**, 3380 (2008).
[7]F. Mompiou, M. Legros, A. Boé, M. Coulombier, J.-P. Raskin, and T. Pardoen, Acta Mater. **61**, 205 (2013).
[8]W. C. Carter and A. M. Glaeser, Acta Metall. **35**, 237 (1987).
[9]J. Rödel and A. M. Glaeser, J. Am. Ceram. Soc. **73**, 592 (1990).
[10]H. Yamamoto, Int. J. Fract. **14**, 347 (1978).
[11]R. W. Hertzberg, *Deformation and Fracture Mechanics of Engineering Materials* (John Wiley & Sons, 1996).
[12]M. Aramfard and C. Deng, Sci. Rep. **5**, 14215 (2015).
[13]T. K. Gupta, J. Am. Ceram. Soc. **59**, 259 (1976).
[14]A. M. Thompson, H. M. Chan, M. P. Harmer, and R. E. Cook, J. Am. Ceram. Soc. **78**, 567 (1995).
[15]F. F. Lange and T. K. Gupta, J. Am. Ceram. Soc. **53**, 54 (1970).
[16]G. Q. Xu and M. J. Demkowicz, Phys. Rev. Lett. **111**, 145501 (2013).
[17]I. Adlakha, M. A. Tschopp, and K. N. Solanki, Mater. Sci. Eng. A **618**, 345 (2014).
[18]P. Gumbsch, Mater. Sci. Eng. A **260**, 72 (1999).
[19]F. Sansoz and J. F. Molinari, Scr. Mater. **50**, 1283 (2004).
[20]D. Farkas, S. Van Petegem, P. M. Derlet, and H. Van Swygenhoven, Acta Mater. **53**, 3115 (2005).
[21]Y. Wei, H. Gao, and A. F. Bower, J. Mech. Phys. Solids **57**, 1865 (2009).
[22]C. B. Cui and H. G. Beom, J. Mater. Sci. **49**, 8355 (2014).
[23]S.-W. Kim, H. B. Chew, and K. S. Kumar, Scr. Mater. **68**, 154 (2013).
[24]I. Adlakha, M. Bhatia, K. Solanki, and M. Tschopp, Philos. Mag. **94**(30), 3445 (2014).
[25]S. Plimpton, J. Comput. Phys. **117**, 1 (1995).
[26]P. L. Williams, Y. Mishin, and J. C. Hamilton, Model. Simul. Mater. Sci. Eng. **14**, 817 (2006).
[27]M. I. Mendelev, M. J. Kramer, C. A. Becker, and M. Asta, Philos. Mag. **88**, 1723 (2008).
[28]G. Grochola, S. P. Russo, and I. K. Snook, J. Chem. Phys. **123**, 204719 (2005).
[29]Y. Mishin, M. J. Mehl, D. A. Papaconstantopoulos, A. F. Voter, and J. D. Kress, Phys. Rev. B **63**, 224106 (2001).
[30]M. I. Mendelev, M. J. Kramer, S. G. Hao, K. M. Ho, and C. Z. Wang, Philos. Mag. **92**, 4454 (2012).
[31]S. Nosé, J. Chem. Phys. **81**, 511 (1984).
[32]W. G. Hoover, Phys. Rev. A **31**, 1695 (1985).
[33]J. Li, Model. Simul. Mater. Sci. Eng. **11**, 173 (2003).
[34]D. Faken and H. Jónsson, Comput. Mater. Sci. **2**, 279 (1994).
[35]D. H. Tsai, J. Chem. Phys. **70**, 1375 (1979).
[36]F. J. Humphreys and M. Hatherly, *Recrystallization and Related Annealing Phenomena* (Elsevier, 2012).
[37]T. Sakai, A. Belyakov, R. Kaibyshev, H. Miura, and J. J. Jonas, Prog. Mater. Sci. **60**, 130 (2014).
[38]M. R. Drury and F. J. Humphreys, Acta Metall. **34**, 2259 (1986).
[39]M. Umemoto, Mater. Trans. **44**, 1900 (2003).
[40]J. W. Cahn, Y. Mishin, and A. Suzuki, Acta Mater. **54**, 4953 (2006).
[41]See supplementary material at http://dx.doi.org/10.1063/1.4942842 for movies of the detailed crack-SCGBM processes.
[42]A. Stukowski, Model. Simul. Mater. Sci. Eng. **18**, 015012 (2010).
[43]M. Aramfard and C. Deng, Model. Simul. Mater. Sci. Eng. **22**, 055012 (2014).
[44]T. Frolov, S. V. Divinski, M. Asta, and Y. Mishin, Phys. Rev. Lett. **110**, 255502 (2013).
[45]T. Frolov, D. L. Olmsted, M. Asta, and Y. Mishin, Nat. Commun. **4**, 1899 (2013).
[46]H. Miura, IOP Conf. Ser. Mater. Sci. Eng. **89**, 012007 (2015).
[47]M. Griffiths, AECL Nucl. Rev. **2**, 1 (2013).